

# Discovery of an X-ray selected radio-loud obscured AGN at $z=1.246$

X. Barcons<sup>1</sup>, R. Carballo<sup>1,2</sup>, M.T. Ceballos<sup>1</sup>, R.S. Warwick<sup>3</sup>, J.I. González-Serrano<sup>1</sup>

<sup>1</sup> Instituto de Física de Cantabria (Consejo Superior de Investigaciones Científicas - Universidad de Cantabria), 39005 Santander, Spain

<sup>2</sup> Departamento de Física Moderna, Universidad de Cantabria, 39005 Santander, Spain

<sup>3</sup> Department of Physics and Astronomy, University of Leicester, Leicester LE1 7RH, UK

17 July 1998

## ABSTRACT

We have discovered an obscured active galaxy at redshift  $z = 1.246$  identified with the *ROSAT* X-ray source RX J1011.2+5545. We report on multiwavelength observations of this source and discuss its X-ray, optical and radio properties. This is the first X-ray selected, obscured active galaxy at high redshift to be shown to be radio-loud, with a radio counterpart exhibiting a classical double-lobe morphology.

**Key words:** Galaxies: active, X-rays: galaxies, Radio Continuum: galaxies

## 1 INTRODUCTION

Deep X-ray surveys have recently revealed a population of moderately to heavily absorbed active galactic nuclei (AGN) at faint fluxes. A few such objects are known to be at high redshift, for example one source discovered by *ROSAT* is at  $z=2.35$  (Almaini et al 1995) and two others discovered by *ASCA* have  $z=0.9$  and  $z=0.672$  (Ohta et al 1996; Boyle et al 1998). The so-called Narrow-Line X-ray Emitting Galaxies (NLXGs) might, in fact, be the low redshift counterparts of these obscured objects, since both classes are characterised by hard X-ray spectra (Carballo et al 1995; Almaini et al 1996). The discovery of such sources at faint X-ray fluxes is of vital importance in explaining the origin of the X-ray background, since the brightest AGN in the X-ray sky (mostly type 1 AGN) generally have much softer X-ray spectra than the X-ray background spectrum (Fabian & Barcons 1992).

The UK *ROSAT* Medium Sensitivity Survey (Branduardi - Raymond et al 1994; Carballo et al 1995) was carried out in order to identify a complete sample of moderately faint X-ray selected sources (flux over the 0.5–2 keV band in excess of  $1.7 \times 10^{-14} \text{ erg cm}^{-2} \text{ s}^{-1}$ ) over a significant area of the sky ( $2.2 \text{ deg}^2$ ) in a region of minimal Galactic absorption. In this survey the source with the highest hardness ratio is RX J1011.2+5545 with  $HR = 0.67$  ( $HR = (H - S)/(H + S)$  where  $S$  and  $H$  are the counts in PSPC channels 11–39 and 40–200 respectively). It is also one of its brightest sources with a flux  $S(0.5 - 2 \text{ keV}) = 6.6 \times 10^{-14} \text{ erg cm}^{-2} \text{ s}^{-1}$ . The hard X-ray spectrum together with the fact that the source has no optical counterpart visible on the POSS plates (which is atypical of the X-ray sources at this flux level), suggested a possibly highly

obscured source and prompted us to start a program of follow-up optical and *ASCA* hard X-ray observations. A NED search also revealed that the source is a radio-emitter at various frequencies, with a double lobe morphology. The combination of radio, optical and X-ray data has enabled us to classify this object as a radio-loud, moderately obscured, high-excitation AGN at a redshift  $z = 1.246$ . This is the first X-ray selected obscured AGN discovered at high redshift found to be radio loud. In this paper we report on all of the recent observations and discuss the nature of this source.

## 2 THE DATA

### 2.1 *ROSAT* soft X-ray observations

The discovery observation was carried out on May 11, 1992 with the *ROSAT* PSPC-B, giving an exposure time of 18529s. The data were reduced and scanned for sources as described in Carballo et al (1995). After a number of sources in the PSPC image were identified with optical counterparts, the astrometry of the X-ray field was corrected by applying shifts in RA and DEC. The final X-ray position for the source RX J1011.2+5545 is  $10^{\text{h}} 11^{\text{m}} 12^{\text{s}}.4$  and  $55^{\circ} 44' 50''$  (J2000) with a 90 per cent error circle of radius  $\sim 4''$ . The X-ray image showed no evidence for any extension in the source (the FWHM is  $27''$ , consistent with the PSF at an offset angle from the *ROSAT* field centre of  $7.3'$ ). The Galactic column density in this direction is  $6.7 \times 10^{19} \text{ cm}^{-2}$ .

We used the FTOOLS/XSELECT V3.6 package to extract the counts contained within a circle of radius  $1.5'$  centered on the source and used a “source-free” region of radius  $6.5'$  at a similar off-axis angle in the background subtraction. For the purpose of spectral fitting we grouped the PSPC

arXiv:astro-ph/9810041v1 2 Oct 1998

pulse-height data so that every spectral bin contained at least 20 counts, leading to a 0.1–2.0 keV source spectrum with just 6 bins.

A single power-law fit, assuming only Galactic line-of-sight absorption, gives a very flat photon spectral index  $\Gamma = 0.93^{+0.20}_{-0.23}$  (we always quote 90 per cent errors for a single parameter). However, the quality of the fit is not very good ( $\chi^2/\nu = 10.2/4$ ) corresponding to probability for the null hypothesis (PNH) of only 3.7 per cent. The inclusion in the spectral model of absorption intrinsic to the X-ray source produces a somewhat better fit ( $\chi^2/\nu = 4.4/3$ ) with a steeper underlying power law (although formally the improvement in the fit is not significant in terms of the F-test). Clearly data at higher energies are required in order to better constrain the continuum slope in this source.

## 2.2 ASCA hard X-ray observations

RX J1011.2+5545 was observed with *ASCA* on November 12–13, 1995. The source was clearly seen in both the SIS0 and SIS1 cameras, which were operated in 1-CCD mode (Bright mode). Standard FTOOLS/XSELECT V3.6 tasks and techniques were used to clean the data (using default parameters), resulting in effective exposure times of 53054s (SIS0) and 52855s (SIS1). In this paper we ignore the GIS2 and GIS3 observations since the source is barely detected in these detectors. We rely on the spectral calibration of the SIS0 data, in preference to that for SIS1 when necessary.

A spectrum was extracted from a 3' radius region centred on the source. The background subtraction was found to be much more accurate when we chose a source-free region within the same image rather than using the available archival background images. (For example, a detector Fe fluorescent line in the 6–7 keV spectral region went away when we used the adopted method, but not when the archival background was used). After background subtraction the resulting spectrum was again binned in order to give a minimum of 20 counts per spectral channel. The result was 16 bins for SIS0 and 15 for SIS1. No significant source variability was found in the data.

The simultaneous fitting of the SIS0 and SIS1 data with a single power-law model (but with different normalisations applying to the two detectors to allow for calibration uncertainties) gives an acceptable fit ( $\chi^2/\nu = 34.5/28$  with PNH of 18.5 per cent) with a rather flat photon index  $\Gamma = 1.43^{+0.24}_{-0.23}$ . The inclusion of absorption intrinsic to the X-ray source again produces a steeper underlying power law but with only a modest improvement in the fit ( $\chi^2/\nu = 31.8/27$ ) (which again is not a significant improvement in terms of the F-test).

We then combined the *ROSAT* and *ASCA* data so as to better constrain the spectral parameters. Our approach has been to assume the same value of the model normalisation for the *ROSAT* and *ASCA* SIS0 data but allow a different normalisation for *ASCA* SIS1 data. This procedure produces a significantly better fit than taking the same normalisation for all three datasets (at 99.9 per cent using F-test), whereas introducing different normalisations for each instrument does not result in a significant improvement. A single power law fit is only marginally acceptable ( $\chi^2/\nu = 53.9/34$  with a PNH=1.6 per cent), with  $\Gamma = 1.13 \pm 0.16$ . However, the fit improves if absorption intrinsic to the source

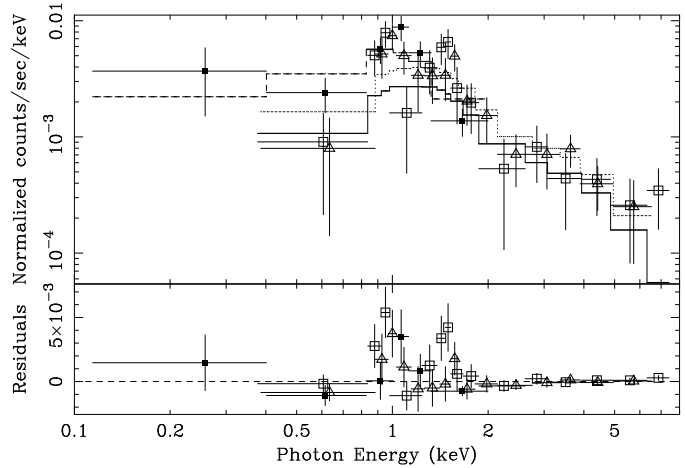


**Figure 1.** The measured *ROSAT* and *ASCA* X-ray spectra of RX J1011.2+5545 together with the residuals to the best fitting (power-law plus intrinsic absorption) model. The filled squares, empty squares and triangles are the *ROSAT* PSPC, the *ASCA* SIS0 and the *ASCA* SIS1 data points respectively. The *ROSAT* PSPC model is shown with a dashed line, the *ASCA* SIS0 one with a solid line and the *ASCA* SIS1 one with a dotted line.

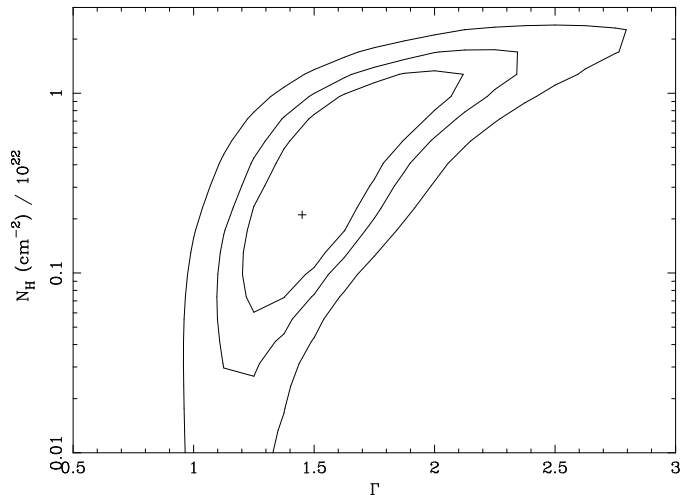


**Figure 2.** Confidence contours (68, 90 and 99 per cent confidence) for the intrinsic absorption and photon index from the combined *ROSAT* and *ASCA* data.

is included ( $\chi^2/\nu = 47.2/33$  with PNH of 5.2 per cent). The best fit (see Fig. 1) corresponds to  $\Gamma = 1.45^{+0.72}_{-0.28}$  and  $N_H = (2.1^{+12.4}_{-1.6}) \times 10^{21} \text{ cm}^{-2}$  (at the redshift of the source  $z = 1.246$ ). Fig. 2 shows the confidence contours for the two free spectral parameters.

There is some evidence for significant residuals in all three instruments at  $\sim 1$  keV (Fig. 1). The inclusion of a Gaussian-line component centered at this energy results in a further improvement of the fit ( $\chi^2/\nu = 31.8/29$ ). However, it is not completely obvious that such a feature is associated with the source; the corresponding rest-frame energy is  $2.2 \pm 0.1$  keV with a rest-frame equivalent width  $\sim 165$  eV. One could identify this as a SiXIV–SiXVI complex (Netzer & Turner 1997), but then the Fe K line should be seen in the spectrum and it is not (rest-frame equivalent width  $< 418$  eV at 95 per cent confidence). Attempts to account for these

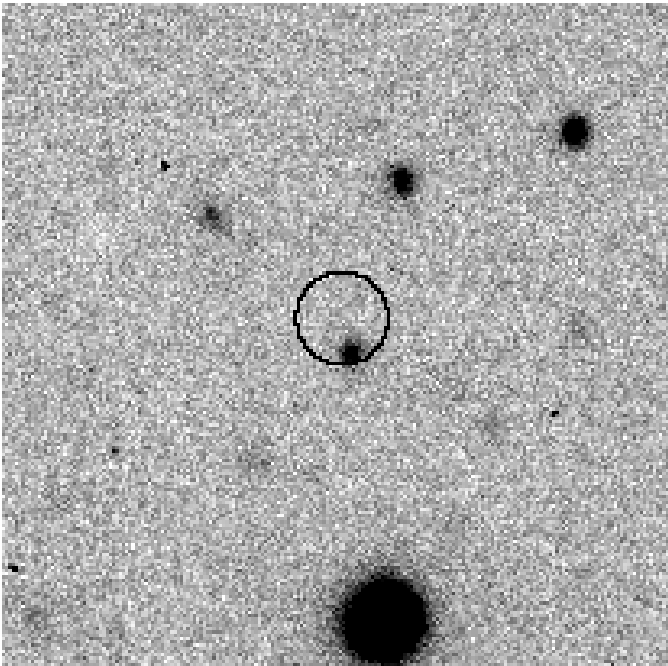


**Figure 3.** *R*-band image of the field around RX J1011.2+5545. The image is 1 arcmin each side. The circle is the 90 per cent error circle for the *ROSAT* X-ray position

residuals in the X-ray spectrum in terms of ionised absorbers did not show significant improvement in the fit.

We conclude that the absorbed, power-law fit is the most tenable model. The flux of the source is  $S(0.5 - 2 \text{ keV}) = 6.6 \times 10^{-14} \text{ erg cm}^{-2} \text{ s}^{-1}$  and  $S(2 - 10 \text{ keV}) = 1.9 \times 10^{-13} \text{ erg cm}^{-2} \text{ s}^{-1}$  and the K-corrected rest frame luminosity (using the measured redshift of  $z = 1.246$ ) is  $L(0.5 - 2 \text{ keV}) = 4.8 \times 10^{44} \text{ erg s}^{-1}$  and  $L(2 - 10 \text{ keV}) = 2.1 \times 10^{45} \text{ erg s}^{-1}$  ( $H_0 = 50 \text{ km s}^{-1} \text{ Mpc}^{-1}$  and  $q_0 = 0$ ).

### 2.3 Optical imaging

The POSS plates show no counterpart within or near the position of the *ROSAT* source. In order to search for fainter candidate optical counterparts, we imaged the field (as for all the other survey sources) with the CCD camera at the Cassegrain focus of the 2.2m telescope of the Centro Astronómico Hispano Alemán, Calar Alto on February 10, 1994. A single exposure of 900s was taken with the Johnson R filter. The photometric conditions were good and the seeing was  $\sim 1.4''$ . Data reduction and the astrometric and photometric calibrations were performed as described by Carballo et al (1995).

The R-band image (Fig. 3) reveals a single  $R = 21.02 \pm 0.08$  source within or near the error circle of the X-ray source, whose position is  $10^h 11^m 12^s.3$  and  $55^\circ 44' 47''$  (J2000) and is the likely counterpart, later confirmed by spectroscopy. The surface brightness profile of the source does not show compelling evidence for any additional extension to the profile of a bright star.

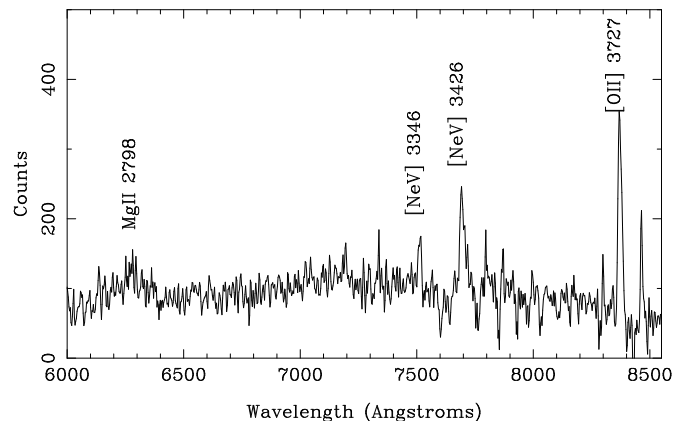
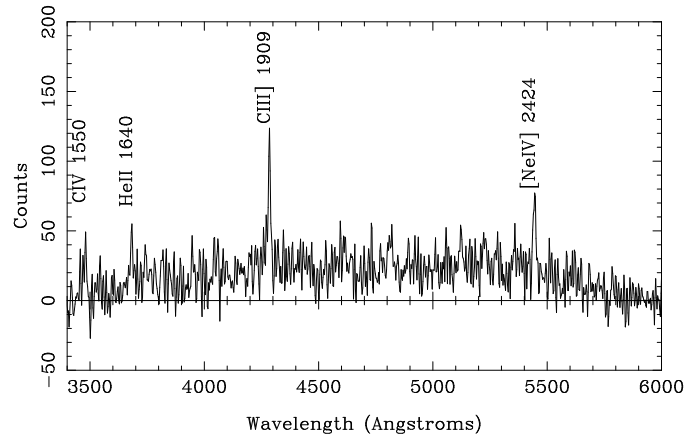


**Figure 4.** Raw optical spectrum of RX J1011.2+5545.

### 2.4 Optical spectroscopy

Optical spectroscopy of the candidate counterpart was carried out at the 4.2m William Herschel Telescope on the Observatorio del Roque de los Muchachos (La Palma) with the ISIS double spectrograph, on February 25, 1998. We used the 150 lines/mm gratings and TEK CCD detectors for both arms, covering a spectral range from 3400 to 8550Å. The atmospheric conditions were very poor with bad and variable sky transparency, dust and seeing, with the latter starting at  $3.5''$  but later improving to between  $2''$  and  $2.5''$ . Two sets of observations were carried out, the first set corresponding to the period of worst seeing with a slit width of  $2.5''$  and the second set with a slit width of  $1.5''$ . Here we ignore the first set of observations, although qualitatively they reveal much the same as the second set.

The observations with the slit width set at  $1.5''$  totalled 5 on-source exposures of 1800s each, all close to parallactic angle and with airmass less than 1.2. The data were reduced using standard IRAF routines. The optimally extracted source spectra were registered to a common wavelength origin using the sky spectrum. The resulting summed spectrum was wavelength calibrated using polynomial fits to standard arc maps, yielding rms residuals of  $0.72\text{Å}$  and  $0.37\text{Å}$  in the blue and in the red respectively. The spectral resolution was measured from unblended arc lines to be  $9.6\text{Å}$  and  $8.8\text{Å}$  in the blue and in the red respectively. Given the poor conditions, no attempt was made to flux calibrate the spectra.

**Table 1.** Detected emission lines in the optical spectrum

Emission line	Redshift	$W_{\lambda}^a$ ( $\text{\AA}$ )	FWHM ( $\text{km s}^{-1}$ )
CIV $\lambda$ 1550	1.2450	35 <sup>b</sup>	< 2500 <sup>b</sup>
HeII $\lambda$ 1640	1.2452	15 <sup>b</sup>	< 800 <sup>b</sup>
CIII] $\lambda$ 1909	1.2445	16	385 <sup>+390</sup> <sub>-380</sub>
[NeIV] $\lambda$ 2423	1.2469	12	560 <sup>+280</sup> <sub>-270</sub>
MgII $\lambda$ 2798	1.242 <sup>b</sup>	15 <sup>b</sup>	2000 <sup>+2700</sup> <sub>-1000</sub> ( <sup>b</sup> )
[NeV] $\lambda$ 3346	1.2453	4	480 <sup>+160</sup> <sub>-130</sub>
[NeV] $\lambda$ 3426	1.2462	14	920 <sup>+310</sup> <sub>-240</sub>
[OII] $\lambda$ 3727	1.2462	42	625 <sup>+60</sup> <sub>-55</sub>

<sup>a</sup> Rest-frame equivalent width<sup>b</sup> Highly uncertain

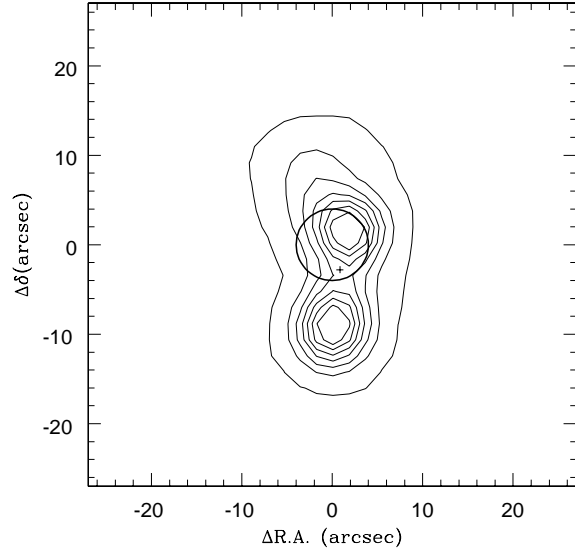
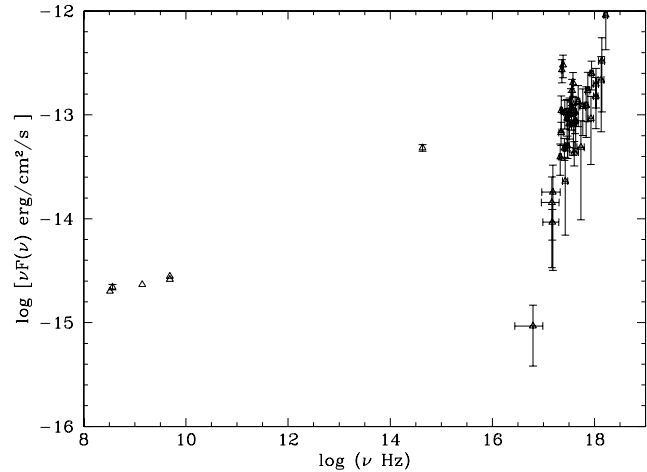
Fig. 4 shows the resulting spectra with markers on the most prominent emission lines. The redshift  $z = 1.246$  has been determined from the strongest features [NeV] $\lambda$ 3426 and [OII] $\lambda$ 3727, although the other emission lines are entirely consistent with this redshift. The presence of the high ionisation [NeV] $\lambda$ 3346 and  $\lambda$ 3426 lines clearly reveals an AGN. Table 1 lists the emission features detected in the spectrum, rest-frame equivalent widths and FWHM estimated via gaussian fitting with 90 per cent errors and corrected for spectral dispersion.

The semi-forbidden CIII] line is clearly detected and narrow (see Table 1). Since this line is predicted to be broad in a type 1 AGN, the implication is that the broad-line region in this AGN is obscured. The CIV and HeII lines appear also narrow, but in a low signal to noise part of the spectrum. The MgII line is probably broad, but with an equivalent width normalised to the equivalent width of the narrow lines significantly smaller (10–20 times) than is typically found in type 1 AGN (Francis et al 1991). Broad MgII has been found in IR hyperluminous galaxies (Hines & Wills 1993; Hines et al 1995) and high-redshift radiogalaxies (di Serego Alighieri, Cimati & Fosbury 1994; Stockton, Kellogg & Ridgway 1995) and has been interpreted as scattered emission from a hidden type 1 AGN.

## 2.5 Radio data

We searched in various archives for radio observations of our source. There are a number of detections, the most relevant of which are the Westerbork Northern Sky Survey (Rengelink et al 1997) at 326 MHz, the Texas Survey (Douglas et al 1996) at 365 MHz, the FIRST survey (White et al 1997) at 1.4 GHz and the Green Bank 6cm survey (Gregory et al 1996) at 4.85 GHz. Both the Texas and the FIRST surveys resolve the source into two components aligned approximately N-S. The N component is the brightest in the FIRST data (0.090 Jy compared to the 0.071 Jy of the S component). The optical position lies in between both components (see Fig. 5). The separation between the components is  $\sim 11''$  at 1.4 GHz and  $\sim 15''$  at 365 MHz.

The integrated radio fluxes together with the measurements at optical and X-ray frequencies are shown in Fig. 6 in the form of a spectral energy distribution. The radio spectrum has a  $S_{\nu} \propto \nu^{-0.9}$  shape from 326 MHz to 4.85 GHz,

**Figure 5.** A radio map of RX J1011.2+5545 at 1.4GHz from the FIRST survey. The cross shows the position of the optical source and the thick circle is the error circle of the X-ray source.**Figure 6.** The spectral energy distribution of RX J1011.2+5545 from radio to X-rays (see text for details on the data points).

which is typical of lobe-dominated radio sources. Although from the spatial information at the various frequencies it is not completely clear that this is a lobe-dominated double source, both the spectral index and the position of the optical source strongly support this hypothesis.

## 3 DISCUSSION

There are various facts that support the conclusion that RX J1011.2+5545 is an AGN, the most relevant being a high radio to optical flux ratio, a 2–10 keV luminosity exceeding  $10^{45} \text{ erg s}^{-1}$  and the broad MgII emission. In addition the strong [NeV] $\lambda$ 3624 line implies the presence of an underlying hard ionising continuum.

We initially suspected obscuration in this source because of its high *ROSAT* PSPC hardness ratio. Also for a typical uncovered AGN, the average optical magnitude corresponding to its X-ray flux would be  $R \sim 19$  (see, e.g., Hasinger 1996) instead of the observed value of  $R \sim 21$ . The absence of a broad CIII] line confirms this obscuration hypothesis.

A weak broad MgII line is detected, its equivalent width being 3 to 5 times smaller than for a type I AGN (Francis et al 1991; Baker & Hunstead 1995). This cannot be explained as a simple obscuration effect, since in that case both the broad lines and the nuclear continuum would be equally suppressed, leaving the equivalent widths unchanged. The weakness of MgII and the absence of broad CIV and HeII may be the result of dilution by a source of blue continuum over and above that emanating directly from the nucleus. The requirement would be that at a rest wavelength of  $\sim 2800\text{\AA}$  the nuclear continuum may be only 20 to 50 per cent of the total. The nature of this extra blue component is unknown, but reflected nuclear radiation, nebular continuum and copious star formation are all possibilities. The non-detection of a reflected Fe K line in X-rays and the strong [OII] line with respect to typical type I situation favour the enhanced star formation scenario. The equivalent width of the broad CIII] component is expected to be roughly 2 to 5 times smaller than that of MgII in a type I AGN, and therefore it would be very weak in this object. Obscuration of the nuclear continuum could also lead to the narrow [NeV] lines having enhanced equivalent widths.

The power-law in the X-ray spectrum of this object is similar to that found for other luminous radio-loud quasars at high redshifts, ( $\Gamma \sim 1.5$ , Cappi et al 1997), distinctively flatter than for radio-quiet AGN. This has been associated with different emission mechanisms (synchrotron self-Compton with the radio-emitting electrons in radio-loud AGN versus nuclear emission in radio-quiet objects). It is then possible that in radio-loud active galaxies the line-of-sight to X-ray emitting regions intercepts less obscuring material than does the direct path to the nucleus. Larger absorbing columns ( $N_H \sim 10^{22} \text{ cm}^{-2}$ ) than that observed in RX J1011.2+5545 are common only among radio-loud quasars at very high redshifts ( $z > 3$ , Cappi et al 1997, Fiore et al 1998). The possible contribution to the X-ray flux from a cluster of galaxies hosting this source (which might be dominant in radiogalaxies, Crawford & Fabian 1996) is small, since the X-ray data does not show evidence for a spectral cutoff consistent with thermal emission.

The amount of X-ray absorption predicts an optical extinction for the X-ray source which is  $A_V = 1.1_{-0.85}^{+6.7}$ , using standard dust to gas ratios. For moderate extinction ( $A_V \sim 1 - 2$ ), the nuclear light seen in the optical can be direct radiation from the nucleus. However, if the obscuration is much larger, then the MgII broad line would be seen through reflection only. It is even possible that the nucleus is very heavily obscured in the optical ( $A_V \gg 10$ ) in which case the direct X-ray continuum and nuclear Fe K emission might also be suppressed, leaving a dominant X-ray component arising in the radio lobes with only moderate associated photoelectric absorption. Disentangling both possibilities requires high spatial resolution optical and IR observations.

In any event, the discovery of this object demonstrates that high-redshift radio-loud obscured AGN are present at

faint X-ray fluxes. Such objects may play a role, albeit probably minor, in producing the X-ray background. Surveys to be carried out with AXAF and XMM will undoubtedly find large numbers of obscured AGNs and show what is their contribution to the X-ray background.

## ACKNOWLEDGMENTS

XB and RC were visiting astronomers of the Centro-Astronómico Hispano-Alemán, Calar Alto, operated by the Max-Planck-Institute for Astronomy, Heidelberg jointly with the Spanish ‘Comisión Nacional de Astronomía’. The William Herschel Telescope is operated on the island of La Palma by the Isaac Newton Group in the Spanish Observatorio del Roque de los Muchachos of the Instituto de Astrofísica de Canarias. This research has made use of the NASA/IPAC Extragalactic Database (NED), which is operated by the Jet Propulsion Laboratory, California Institute of Technology under contract with the National Aeronautics and Space Administration. XB, RC, MTC and JIGS acknowledge financial support by the DGES under project PB95-0122.

## REFERENCES

- Almaini O., Boyle B.J., Griffiths R.E., Shanks T., Stewart G.C., Georgantopoulos I., 1995, MNRAS, 277, L31
- Almaini O., Shanks T., Boyle B.J., Griffiths R.E., Roche N., Stewart G.C., Georgantopoulos I., 1996, MNRAS, 282, 295
- Baker J.C., Hunstead R.W., 1995, ApJ, 452, L95. Erratum: ApJ, 468, L131
- Boyle, B.J., Almaini, O., I. Georgantopoulos, A.J. Blair, G.C. Stewart, R.E. Griffiths, T. Shanks, K.F. Gunn, 1998, MNRAS, in the press
- Branduardi-Raymont G. et al. 1994, MNRAS, 270, 947
- Cappi M., Matsuoka M., Comastri, A., Brinkmann W., Elvis M., Palumbo G.G.C., Vignali C., 1997, ApJ, 478, 492
- Carballo R., Warwick R.S., Barcons X., González-Serrano J.I., Barber C.R., Martínez-González E., Pérez-Fournon I., Burgos J., 1995, MNRAS, 277, 1312
- Crawford C.S., Fabian A.C., 1996, MNRAS, 282, 1483
- di Serego Alighieri S., Cimatti A., Fosbury R.A.E., 1994, ApJ, 431, 123
- Douglas J.N., Bash F.N., Boyzan F.A., Torrence G.W., Wolfe C., 1996, AJ, 111, 1945
- Fabian A.C., Barcons X., 1992, ARAA, 30, 429
- Fiore F., Elvis M., Giommi P., Padovani P., 1998, ApJ, 492, 79
- Francis P.J., Hewett P.C., Foltz C.B., Chaffee F.H., Weymann R.J., Morris S.L., 1991, ApJ, 373, 465
- Gregory P.C., Scott W.K., Douglas K., Condon J.J., 1996, ApJS, 103, 427
- Hasinger G., 1996, A&AS, 120, 607
- Hines D.C., Schmidt G.D., Smith P.S., Cutri R.M., Low F.J., 1995, ApJ, 450, L1
- Hines D.C., Wills B.J., 1993, ApJ, 415, 82
- Netzer H., Turner T.J., 1997, ApJ, 488, 694
- Ohta K., Yamada T., Nakanishi K., Kohno K., Akiyama M., Kawabe R., 1996, Nat., 382, 426
- Rengelink R.B., Tang Y., De Bruyn A.G., Miley G.K. Bremer M.N., Roettgering H.J.A., Bremer M.A.R., 1997, A&AS, 124, 259
- Stockton A., Kellogg M., Ridgway S.E., 1995, ApJ, 443, L69
- White R.L., Becker R.H., Helfand D.J., Gregg M.D., 1997, ApJ, 475, 479